Environmental Toxicology

WILEY

ENVIRONMENTAL TOXICOLOGY

RESEARCH ARTICLE OPEN ACCESS

Protective Effects of Carvacrol on Mercuric Chloride-Induced Lung Toxicity Through Modulating Oxidative Stress, Apoptosis, Inflammation, and Autophagy

Berna Eriten[1] | Sefa Kucukler[2] | Cihan Gur[3] | Adnan Ayna[4] | Halit Diril[5] | Cuneyt Caglayan[6]

[1]Department of Pathology, Sancaktepe Sehit Prof. Dr. Ilhan Varank Training and Research Hospital, Türkiye | [2]Department of Biochemistry, Faculty of Veterinary Medicine, Atatürk University, Erzurum, Türkiye | [3]Department of Medical Laboratory Techniques, Vocational School of Health Services, Atatürk University, Erzurum, Türkiye | [4]Department of Chemistry, Faculty of Science and Literature, Bingol University, Bingol, Türkiye | [5]Medical Biochemistry Laboratory, Dursun Odabaş Medical Center, Van Yüzüncü Yıl University, Türkiye | [6]Department of Medical Biochemistry, Faculty of Medicine, Bilecik Seyh Edebali University, Bilecik, Türkiye

Correspondence: Berna Eriten (bernaeriten@gmail.com) | Cuneyt Caglayan (cuneyt.caglayan@bilecik.edu.tr)

Received: 29 April 2024 | **Revised:** 10 June 2024 | **Accepted:** 23 July 2024

Funding: The authors received no specific funding for this work.

Keywords: apoptosis | carvacrol | inflammation | lung toxicity | mercuric chloride | oxidative stress

ABSTRACT

Mercuric chloride ($HgCl_2$) is extremely toxic to both humans and animals. It could be absorbed via ingestion, inhalation, and skin contact. Exposure to $HgCl_2$ can cause severe health effects, including damages to the gastrointestinal, respiratory, and central nervous systems. The purpose of this work was to explore if carvacrol (CRV) could protect rats lungs from damage caused by $HgCl_2$. Intraperitoneal injections of $HgCl_2$ at a dose of 1.23 mg/kg body weight were given either alone or in conjunction with oral CRV administration at doses of 25 and 50 mg/kg body weight for 7 days. The study included biochemical and histological techniques to examine the lung tissue's oxidative stress, apoptosis, inflammation, and autophagy processes. $HgCl_2$-induced reductions in GSH levels and antioxidant enzymes (SOD, CAT, and GPx) activity were enhanced by CRV co-administration. Furthermore, MDA levels were lowered by CRV. The inflammatory mediators NF-κB, IκB, NLRP3, TNF-α, IL-1β, IL6, COX-2, and iNOS were all reduced by CRV. When exposed to $HgCl_2$, the levels of apoptotic Bax, caspase-3, Apaf1, p53, caspase-6, and caspase-9 increased, but the levels of antiapoptotic Bcl-2 reduced after CRV treatment. CRV decreased levels of Beclin-1, LC3A, and LC3B, which in turn decreased $HgCl_2$-induced autophagy damage. After $HgCl_2$ treatment, higher pathological damage was observed in terms of alveolar septal thickening, congestion, edema, and inflammatory cell infiltration compared to the control group while CRV ameliorated these effects. Consequently, by preventing $HgCl_2$-induced increases in oxidative stress and the corresponding inflammation, autophagy, apoptosis, and disturbance of tissue integrity in lung tissues, CRV might be seen as a useful therapeutic alternative.

1 | Introduction

Heavy metals have been reported as elements that have a high density and could be toxic or harmful to human and other creatures at certain concentrations [1, 2]. Lead, mercury, cobalt, cadmium, arsenic, and chromium are a few examples of heavy metals [3]. Although the Earth's crust contains these elements naturally, human activities including mining, industrial processes, and inappropriate waste disposal also release them into the environment [4]. At present, pollution caused by metal is commonly led by mining, urban wastes, industrial sewage, fossil fuel residues, acid rain, fertilizers, and pesticides [5].

Mercuric chloride is a chemical made of mercury and chlorine that is often referred to as mercury (II) chloride ($HgCl_2$) [6]. It has been used historically in fungicides, disinfectants, and as a reagent in laboratory settings [7]. However, because of its toxicity and detrimental effects on health, its use has decreased. $HgCl_2$ exposure can happen by skin contact, ingestion, or inhalation. It can lead to serious health issues that influence the skin, kidneys, and neurological system. Frequent or prolonged exposure to high concentrations of $HgCl_2$ can cause symptoms like renal damage, respiratory troubles, gastrointestinal disorders, tremors, and in extreme situations, even death [8].

Breathing in dust particles or vapors containing $HgCl_2$ might cause lung problems in the long run as well as acute respiratory distress. Inhaling $HgCl_2$ can irritate the respiratory system and result in symptoms including coughing and dyspnea [9]. Extended exposure to elevated $HgCl_2$ concentrations may lead to more serious lung complications, such as chemical pneumonia, pulmonary edema, and pneumonitis, which are inflammations of the lung tissue. Inhaling $HgCl_2$ over an extended period of time can cause respiratory problems like chronic bronchitis, reduced lung function, and fibrosis [10]. Reducing exposure to $HgCl_2$ is essential to avoid respiratory issues. Thus, in cases of $HgCl_2$-induced toxicity, it is preferable to investigate appropriate treatment opportunities with a plant origin that might alleviate against toxicities caused by $HgCl_2$.

Carvacrol (CRV) is a natural monoterpenoid phenol, which is commonly identified in essential oils, particularly in oregano oil and thyme oil [11]. It is widely used as a flavor, fragrance, and preservative in food or cosmetics [12, 13]. Recently, important explorations have been performed to determine the pharmacological and biological effects of CRV in clinical applications [14]. Studies indicate that CRV has antioxidant, anticancer, anti-inflamatory, antiapoptotic, and antimicrobial activities [11, 15–17]. CRV's ability to prevent lung toxicity caused by $HgCl_2$ has not been thoroughly studied, though. Therefore, this study aimed to assess the potential utility of CRV as an herbal remedy to protect rats from lung impairment caused by $HgCl_2$.

2 | Materials and Methods

2.1 | Chemicals

Carvacrol (98%) and $HgCl_2$ (99.5%) were obtained from Sigma-Aldrich (St. Louis, MO, USA). All of the other compounds and chemical reagents utilized in the current research were of analytical grade.

2.2 | Animals

Thirty-five Wistar albino rats (10–12 weeks, 220–250 g) were used in the experimental procedures. All rats had unlimited access to water and a standard rat diet throughout this study. The rats were housed in a standard environment with a room temperature of 24 ± 1°C, humidity level of 45% ± 5%, and 12 h light–dark cycle. The experiment protocol was approved by the Animal Experiments Local Ethics Committee of the Ataturk University (Approval No: 2023–9/146).

2.3 | Experimental Design

The treated dosages of CRV and $HgCl_2$ have been determined from our previously published studies [11, 18]. The rats were arbitrarily divided in five groups of seven rats. Every group received treatment for 7 days in a row.

(I) Control group: physiological saline was orally given to rats.

(II) CRV group: CRV (50 mg/kg, b. w.) was orally given to rats.

(III) $HgCl_2$ group: $HgCl_2$ (1.23 mg/kg, b. w.) was administered intraperitoneally (i.p.).

(IV) $HgCl_2$ + CRV 25 group: $HgCl_2$ (1.23 mg/kg, b. w.) was administered intraperitoneally (i.p.). Thirty minutes later, CRV (25 mg/kg, b. w.) was orally given to rats.

(V) $HgCl_2$ + CRV 50 group: $HgCl_2$ (1.23 mg/kg, b. w.) was administered intraperitoneally (i.p.). Thirty minutes later, CRV (50 mg/kg, b. w.) was orally given to rats.

Rats were given mild sevoflurane anesthesia and decapitated (sevorane liquid 100%, Abbott Laboratory, Istanbul, Türkiye) 24 h after the last administration (on the 8th day). A portion of the lung tissues was stored at − 80°C until biochemical and molecular analyses. The remaining part of the lung tissues was fixed in 10% buffered formalin solution for pathological analysis.

2.4 | Lipid Peroxidation and Oxidative Stress Biomarker

The lung tissues were homogenized in a homogenizer in a solution of 1.15% KCl to produce the homogenate. Levels of malondialdehyde (MDA), an indicator of lipid peroxidation, were measured according to Placer, Cushman, and Johnson [19]. Superoxide dismutase (SOD) activity was determined by Sun, Oberley, and Li [20], catalase (CAT) activity by Aebi [21] method, glutathione peroxidase (GPx) activity by Lawrence and Burk [22], and glutathione (GSH) level by Sedlak and Lindsay [23] method. The amounts of GSH and MDA were calculated in nmol/g of tissue. SOD and GPx enzyme activities have been expressed as U/g protein. CAT enzyme activity has been reported as katal/g protein. Protein content of lung tissues was determined by the method developed by Lowry et al. [24].

2.5 | RT-PCR Analyses in Lung Tissues

In the first part of the RT-PCR analyses, total RNAs were isolated from lung tissues. In the total RNA isolation process, 1 mL QIAzol Lysis Reagent (79 306; Qiagen) was added to the tissues and homogenized. Then, 200 μL chloroform was included to the homogenates and vortexed for 15 s. The vortexed solution was centrifuged at 12000 *g* for 15 min, and the topmost translucent phase was shifted to new tubes. Afterwards, 500 μL isopropanol was added to the tubes and centrifuged at 12000 *g* for 10 min. After centrifugation, isopropanol was removed and the pellet was washed with ethyl alcohol. After the ethyl alcohol was removed from the tubes, the pellet was

dissolved with DNase/RNase free water. In the second part of the RT-PCR analyses, RNAs were converted into cDNAs. For this, iScript cDNA Synthesis Kit (Bio-Rad) was used. In these processes, 4 μL 5X iScript Reaction Mix and 1 μL iScript Reverse Transcriptase were added to the RNAs and incubated on the Rotor-Gene Q (Qiagen) device for 5 min at 25°C, 20 min at 46°C, and 1 min at 96°C was incubated. In the third part of the RT-PCR analyses, the synthesized cDNAs were reacted with iTaq Universal SYBR Green Supermix (BIORAD) and the primers whose sequences are given in Table 1. The reaction was carried out on the Rotor-Gene Q (Qiagen) instrument. Temperature and time cycles were performed according to the manufacturer's instructions. After the cycles were completed, genes were normalized to β-Actin using the $2^{-\Delta\Delta CT}$ method [25].

2.6 | Histological Method

To examine histological changes in the lung, the rat tissues were preserved in 10% formalin. Subsequently, sections with 5 μm thickness were extracted from the tissues embedded in paraffin and stained with hematoxylin and eosin (H&E). A binocular Olympus Cx43 light microscope (Olympus Inc., Tokyo, Japan) was used to examine the stained sections, and an EP50 camera was used to take pictures. Damage was assessed blindly for each section. Four independent variables (pathological changes) were scored. Histopathological examination was performed considering pathological changes such as congestion, inflammatory cell infiltration, alveolar septal thickening and edema. In scoring these pathological changes, 0 = negative, 1 = mild, 2 = moderate, 3 = high were used.

2.7 | Statistical Analysis

Biochemical and histological data were statistically analyzed using the package program SPSS 20.0. The "one-way analysis of variance (ANOVA)" test was used to establish statistical differences and significance levels, and the Tukey test was utilized to determine group differences. Results were judged significant at the $p < 0.05$ level, and all data were presented as mean ± standard deviations (SD).

3 | Results

3.1 | Effect of Carvacrol on $HgCl_2$-Induced Lung Oxidative Stress

The antioxidant (SOD, CAT, GPx, and GSH) and oxidant (MDA) markers analyzed in lung tissue are presented in Figure 1. It was determined that $HgCl_2$ treatment reduced antioxidant capacity by decreasing SOD, CAT, and GPx activities and GSH levels ($p < 0.05$). Additionally, MDA levels were found to be higher in the $HgCl_2$ supplement group as compared with the control group ($p < 0.05$). Nevertheless, when CRV plus $HgCl_2$ was administered, MDA levels were considerably reduced, whereas SOD, CAT, and GPx activities, as well as GSH levels, were elevated in comparison to the group that was only given $HgCl_2$ treatment.

3.2 | Effect of Carvacrol on $HgCl_2$-Induced Lung Apoptosis

The protective effects of CRV against $HgCl_2$-induced lung toxicity were assessed through analysis of apoptotic markers Bax, Bcl-2, Apaf-1, p53, caspase-3, caspase-6, and caspase-9. The data obtained show that $HgCl_2$-induced group triggered apoptosis by up-regulating mRNA transcript levels of Bax, Apaf1, p53, caspase-3, caspase-6, and caspase-9 and down-regulating mRNA transcript level of Bcl-2 compared with the control group ($p < 0.05$). However, CRV treatment significantly modulated the mRNA transcript levels of the above-mentioned parameters compared with the $HgCl_2$ group ($p < 0.05$, Figures 2 and 3).

3.3 | Effect of Carvacrol on $HgCl_2$-Induced Lung Inflammation

With the aim of determining the effects of CRV on inflammation, the mRNA transcript levels of NF-κB, IκB, TNF-α, IL-1β, IL-6, NLRP3, COX-2, and iNOS were studied. It was determined that $HgCl_2$ administration caused inflammation in lung tissue and up-regulated the mRNA transcript levels of NF-κB, IκB, TNF-α, IL-1β, IL-6, NLRP3, COX-2, and iNOS ($p < 0.05$). Nevertheless, CRV was found to reduce mRNA transcript levels of above-mentioned parameters in a dose-dependent manner, thereby alleviating inflammation in the lung tissue (Figures 4 and 5).

3.4 | Effect of Carvacrol on $HgCl_2$-Induced JAK2, STAT3, and RAGE Levels

The mRNA transcript levels of JAK2, STAT3, and RAGE in the lung tissue were found increased significantly in $HgCl_2$-treated group in compared with the control group ($p < 0.05$). Administration of both dose of CRV with $HgCl_2$ significantly ($p < 0.05$) decreased in these parameters compared to only $HgCl_2$ group (Figure 6).

3.5 | Effect of Carvacrol on $HgCl_2$-Induced Lung Autophagy

Analysis results of autophagic markers of lung tissue are shown in Figure 7. It was determined that the mRNA transcript levels of Beclin1, LC3A, and LC3B in the lung tissues of $HgCl_2$-treated rats increased compared with the control group ($p < 0.05$). In contrast, CRV administration significantly reduced the levels of these autophagic parameters as compared with $HgCl_2$ alone injected rats.

3.6 | Histopathological Results

Histopathological changes in the lung as a result of $HgCl_2$ and CRV are demonstrated in Figure 8. The control and CRV groups showed less congestion, bleeding, and normal histological structure in terms of alveolar and bronchioles (Figure 8A,B). In the $HgCl_2$ group, thickening of the alveolar septum, an increase in

TABLE 1 | Primer sequences.

Gene	Sequences (5′-3′)	Length (bp)	Accession no.
Bcl-2	F: GACTTTGCAGAGATGTCCAG R: TCAGGTACTCAGTCATCCAC	214	NM_016993.2
Bax	F: TTTCATCCAGGATCGAGCAG R: AATCATCCTCTGCAGCTCCA	154	NM_017059.2
p53	F: GCGCTTCGAGATGTTCCGA R: AGACTGGCCCTTCTTGGTCT	121	NM_030989.3
Apaf-1	F: ACCTGAGGTGTCAGGACC R: CCGTCGAGCATGAGCCAA	192	NM_023979.2
Caspase-3	F: ACTGGAATGTCAGCTCGCAA R: GCAGTAGTCGCCTCTGAAGA	270	NM_012922.2
Caspase-6	F: GAACGAACGGACCTGTGGA R: CAGTCCAGCTCTGTACCTCG	124	NM_012922.2
Caspase-9	F: ACGTGAACTTCTGCCCTTCC R: GGTCGTTCTTCACCTCCACC	117	NM_031632.2
NF-κB	F: AGTCCCGCCCCTTCTAAAAC R: CAATGGCCTCTGTGTAGCCC	106	NM_001276711.1
IκB	F: TCTGAAAGCTGGCTGTGATC R: GCTAAGTGTAGACACGTGTG	180	NM_001105720.2
NLRP3	F: TCCTGCAGAGCCTACAGTTG R: GGCTTGCAGCACTGAAGAAC	185	NM_001191642.1
TNF-α	F: CTCGAGTGACAAGCCCGTAG R: ATCTGCTGGTACCACCAGTT	139	NM_012675.3
IL-1β	F: ATGGCAACTGTCCCTGAACT R: AGTGACACTGCCTTCCTGAA	197	NM_031512.2
IL-6	F: AGCGATGATGCACTGTCAGA R: GGAACTCCAGAAGACCAGAGC	127	NM_012589.2
COX-2	F: AGGTTCTTCTGAGGAGAGAG R: CTCCACCGATGACCTGATAT	240	NM_017232.3
iNOS	F: AGATCAATGCAGCTGTGCTC R: GGCTCGATCTGGTAGTAGTAGA	235	NM_012611.3
JAK2	F: TAGGTACGGAGTATCTCGTG R: TGGAGTTATAGACAGCCAGG	215	NM_031514.1
STAT3	F: TACCTGGAGCAGCTTCATCA R: GATCTCGCCCAAGAGGTTAT	153	NM_012747.2
RAGE	F: CTGAGGTAGGGCATGAGGATG R: TTCATCACCGGTTTCTGTGACC	113	NM_053336.2
Beclin-1	F: TCTCGTCAAGGCGTCACTTC R: CCATTCTTTAGGCCCCGACG	198	NM_053739.2
LC3A	F: GACCATGTTAACATGAGCGA R: CCTGTTCATAGATGTCAGCG	139	NM_199500.2
LC3B	F: GAGCTTCGAACAAAGAGTGG R: CGCTCATATTCACGTGATCA	152	NM_022867.2
β-Actin	F: CAGCCTTCCTTCTTGGGTATG R: AGCTCAGTAACAGTCCGCCT	360	NM_031144.3

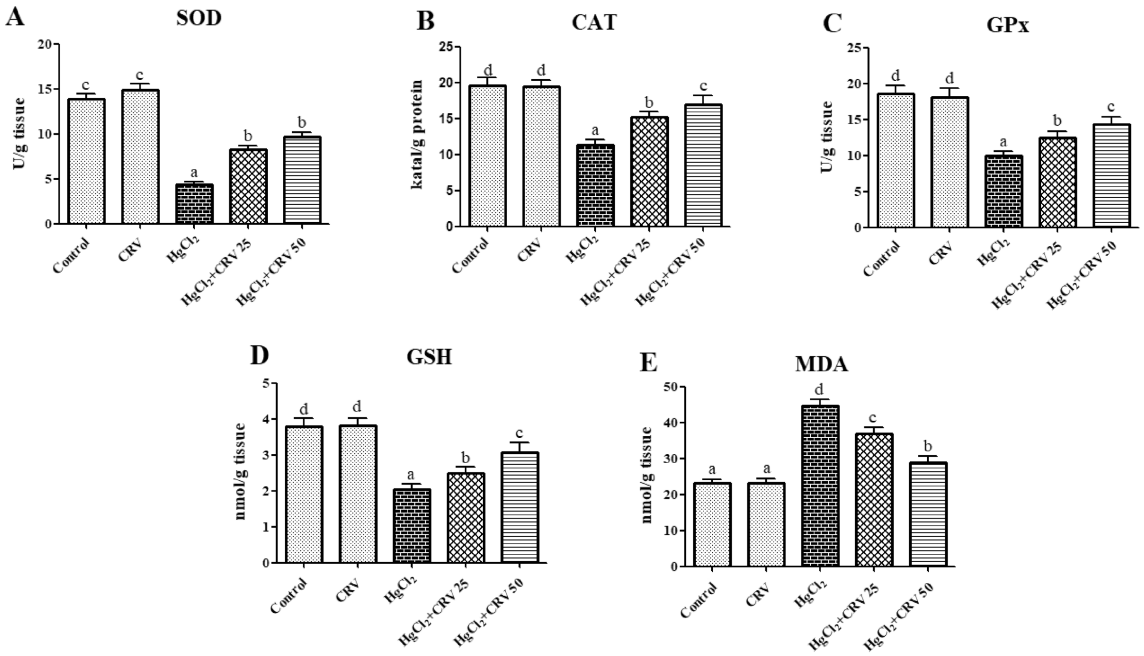

FIGURE 1 | Effects of CRV and $HgCl_2$ treatments on oxidative stress parameters in lung tissue. (A) Ameliorative effect of CRV on $HgCl_2$-induced SOD activity. (B) Ameliorative effect of CRV on $HgCl_2$-induced CAT activity. (C) Ameliorative effect of CRV on $HgCl_2$-induced GPx activity. (D) Ameliorative effect of CRV on $HgCl_2$-induced GSH level. (E) Ameliorative effect of CRV on $HgCl_2$-induced MDA level. Values are expressed as mean ± SD. Different letters (a–d) on the columns show a statistical difference ($p < 0.05$).

inflammatory cells, and an increase in vascular congestion and bleeding were observed (Figure 8C). According to the score results of the $HgCl_2$ group, higher pathological damage was observed in terms of alveolar septal thickening, congestion, edema, and inflammatory cell infiltration ($p < 0.05$). Improvement in septal thickening, congestion, bleeding, and inflammation was observed in the $HgCl_2$ + CRV-25 and $HgCl_2$ + CRV-50 groups (Figure 8D,E). Histopathological changes were also scored and analyzed (Figure 8F). Additionally, it was determined that co-administratioon of 25 and 50 mg CRV with $HgCl_2$ caused a significant decrease in the pathological damage score (alveolar septal thickening, congestion, edema, and inflammatory cell infiltration) ($p < 0.05$).

4 | Discussion

Mercury is released by several industrial processes, such as the production of batteries and pesticides, as well as natural phenomena like volcanic eruptions [26]. It is regarded as one of the most hazardous environmental contaminants that can contaminate soil and water. The possibility that mercury toxicity has harmful effects in adult human and animal body tissues, including neurological, respiratory, renal, dermatological, immunological, reproductive, and developmental diseases, is extremely concerning. Therefore, it is recommended to search for suitable therapy options with a plant origin that may protect against toxicities generated by $HgCl_2$ in situations of $HgCl_2$-induced toxicity. For that reason, the purpose of this study was to determine whether CRV, an herbal treatment, might protect rats' lungs from $HgCl_2$-induced lung damage.

It is well known that $HgCl_2$ produces reactive oxygen species (ROS), which lead to oxidative stress and, ultimately, lipid peroxidation, which destabilizes and fragments the cell membrane [27, 28]. Our findings demonstrate a considerable increase in MDA levels following $HgCl_2$ treatment. Therefore, through increased lipid peroxidation, $HgCl_2$ may produce biochemical and functional alterations in the lung tissues. Additionally, reduced GSH and superoxide radical generation are also connected to the toxicity of $HgCl_2$ [29]. GSH serves as an intracellular antioxidant and mercury carrier because of the thiol (—SH) group. Actually, cells use GSH as their first line of defense when they come into contact with $HgCl_2$-containing materials. Because $HgCl_2$ binds to GSH and then removes it from the cells, the amount of GSH in the cell and its antioxidant capacity are decreased [27]. The current study demonstrated that the lung GSH levels of rats given $HgCl_2$ were considerably lower. Our findings show that pretreatment with CRV considerably ameliorated the raised MDA and decreased GSH levels while protecting rat lung tissue from $HgCl_2$-induced oxidative damage. This could be because CRV has exceptional antioxidant properties. The CAT, GPx, and SOD, components of the enzymatic antioxidant system, guard against ROS and oxidative damage [30]. The restoration of these biochemical markers in the current study showed that CRV could protect the experimental rats' lung from harm caused by exposure to $HgCl_2$. The significant antioxidant activity of CRV, demonstrated by its capacity to protect the lipid cell membrane from oxidation, decrease lipid peroxidation, and increase the levels of antioxidant enzymes, may help to explain our findings.

The natural physiological reaction of cells to various stimuli, infections, or damage—including cytotoxic chemical treatments or radiation therapy—that results in irreversible DNA damages causes apoptosis [31]. The molecular machinery involved in apoptosis is well-characterized and critically depends on the

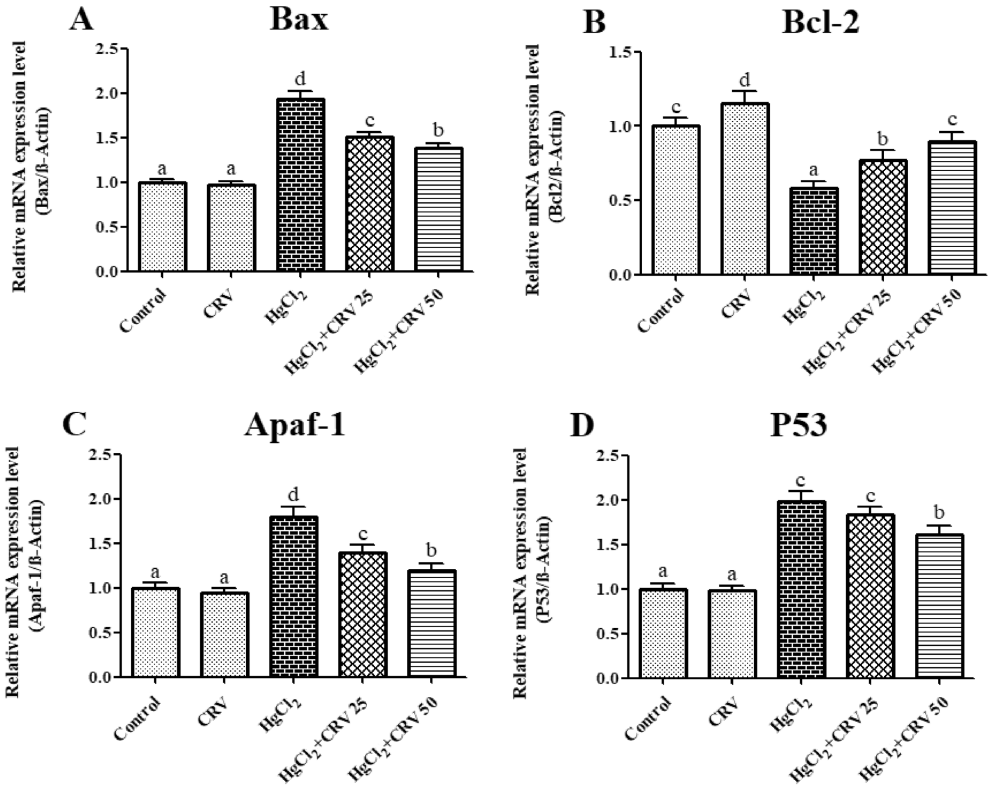

FIGURE 2 | Effects of CRV and $HgCl_2$ treatments on Bax, Bcl-2, Apaf-1, and p53 mRNA transcription levels in lung tissue. (A) Bax mRNA transcript levels, (B) Bcl-2 mRNA transcript level, (C) Apaf-1 mRNA transcript levels, and (D) p53 mRNA transcript levels. Values are expressed as mean ± SD. Different letters (a–d) on the columns show a statistical difference ($p < 0.05$).

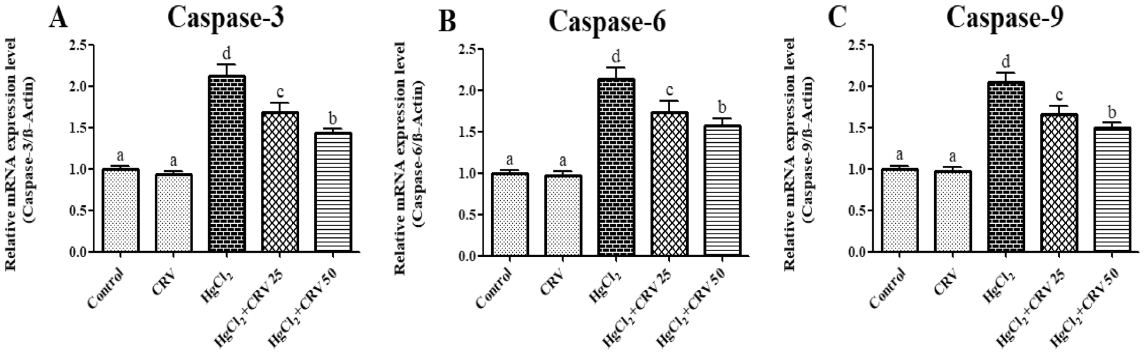

FIGURE 3 | Effects of CRV and $HgCl_2$ treatments on caspase-3, caspase-6, and caspase-9 mRNA transcription levels in lung tissue. (A) caspase-3 mRNA transcript levels, (B) caspase-6 mRNA transcript level, and (C) caspase-9 mRNA transcript levels. Values are expressed as mean ± SD. Different letters (a–d) on the columns show a statistical difference ($p < 0.05$).

activation of caspase proteases. This can be achieved either at the cell surface by activating death receptors or through an intrinsic pathway started by mitochondrial outer membrane permeabilization. The proteins Bax and Bak cause the release of cytochrome c from mitochondria during apoptosis. Upon release, cytochrome c binds to ATP and apoptotic protease activating factor-1 (Apaf-1), which in turn binds to pro-caspase-9 to form an apoptosome, a protein complex [32, 33]. Caspases are cleaved by the apoptosome into their active forms, caspase-9, and caspase-3, respectively, which cleaves and activates procaspase. p53 precludes the cells from duplicating through preventing the cell cycle at G1, or interphase, to bounce the cells phase to healing; nevertheless, it will prompt apoptosis if impairment is extensive and repair efforts be unsuccessful [34]. Our study, similar to earlier ones [29, 35, 36], also showed that $HgCl_2$-induced lung caused apoptosis, as evidenced by the lungs of the $HgCl_2$-treated group having significantly higher levels of Bax, caspase-3, Apaf1, p53, caspase-6, and caspase-9 and lower levels of Bcl-2. $HgCl_2$ can induce cellular apoptosis by transferring cytochrome-c from mitochondria to the cytoplasm, which initiates the caspase pathway and results in the formation of apoptosomes. Rats administered $HgCl_2$ + CRV for treatment

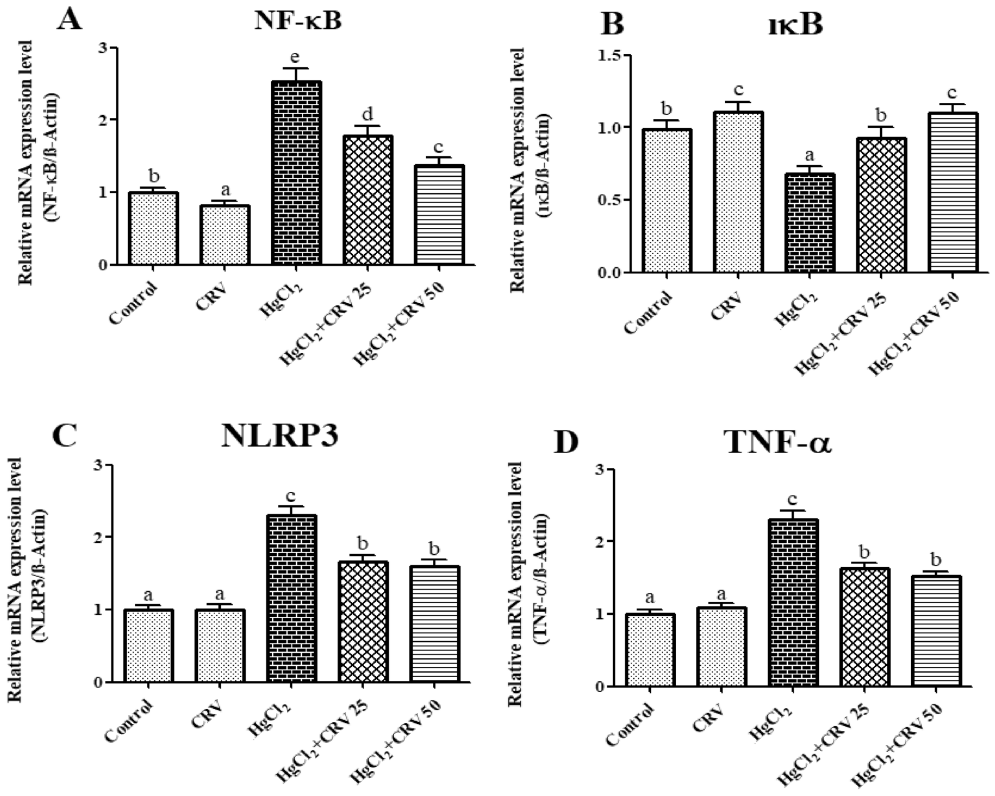

FIGURE 4 | Effects of CRV and $HgCl_2$ treatments on NF-κB, IκB, NLRP3, and TNF-α mRNA transcription levels in lung tissue. (A) NF-κB mRNA transcript levels, (B) IκB mRNA transcript level, (C) NLRP3 mRNA transcript levels, and (D) TNF-α mRNA transcript levels. Values are expressed as mean ± SD. Different letters (a–e) on the columns show a statistical difference ($p < 0.05$).

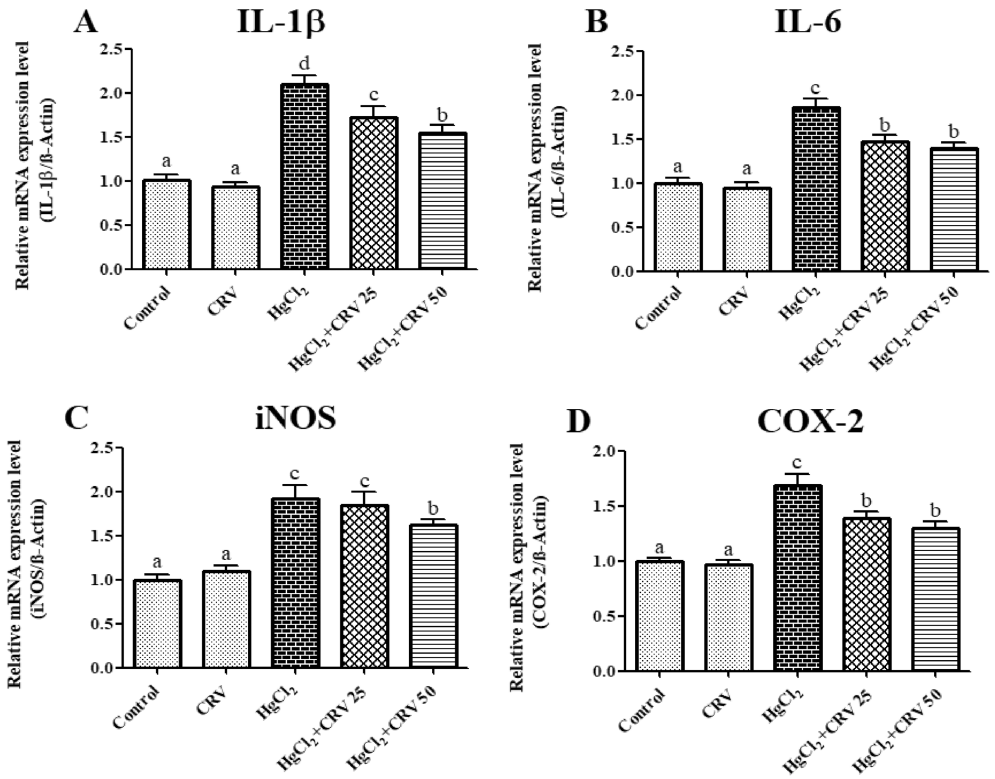

FIGURE 5 | Effects of CRV and $HgCl_2$ treatments on IL-1β, IL-6, iNOS, and COX-2 mRNA transcription levels in lung tissue. (A) IL-1β mRNA transcript levels, (B) IL-6 mRNA transcript level, (C) iNOS mRNA transcript levels, (D) COX-2 mRNA transcript levels. Values are expressed as mean ± SD. Different letters (a–d) on the columns show a statistical difference ($p < 0.05$).

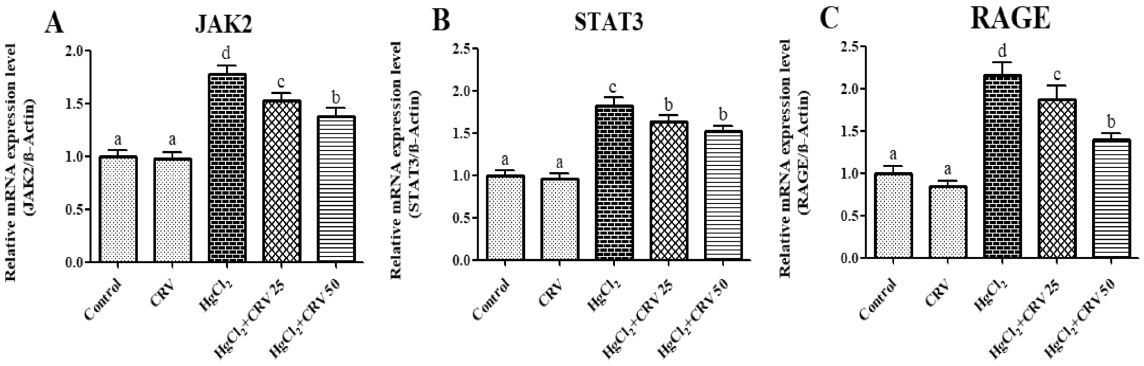

FIGURE 6 | Effects of CRV and $HgCl_2$ treatments on JAK2, STAT3, and RAGE mRNA transcription levels in lung tissue. (A) JAK2 mRNA transcript levels, (B) STAT3 mRNA transcript level, (C) RAGE mRNA transcript levels. Values are expressed as mean ± SD. Different letters (a–d) on the columns show a statistical difference ($p < 0.05$).

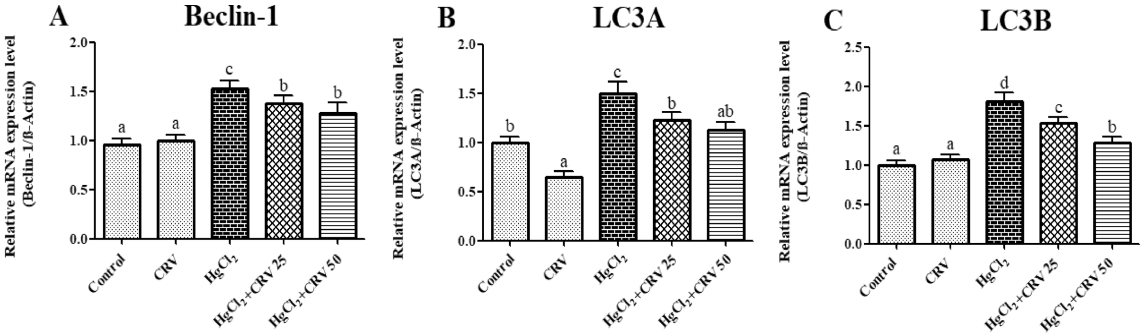

FIGURE 7 | Effects of CRV and $HgCl_2$ treatments on Beclin-1, LC3A, and LC3B mRNA transcription levels in lung tissue. (A) Beclin-1 mRNA transcript levels, (B) LC3A mRNA transcript level, and (C) LC3B mRNA transcript levels. Values are expressed as mean ± SD. Different letters (a–d) on the columns show a statistical difference ($p < 0.05$).

showed a considerable decrease in apoptotic markers in their lungs as compared with the $HgCl_2$-treated group. In an investigation, CoQ10NPs increased the level of Bcl-2 and decreased the amounts of Bax and caspase-3 to prevent hepatorenal apoptosis induced by $HgCl_2$ [36]. In a study, CRV regulated the protein expression of Bcl-2, Bax, caspase-3, and p-ERK impling that CRV has antiapoptotic properties that mitigate ethanol-mediated hippocampus neuronal damage [37]. Another study reported that the levels of apoptotic Bax and caspase-3 increased when exposed to $HgCl_2$, but the levels of antiapoptotic Bcl-2 dropped after $HgCl_2$ treatment while CRV treatment reversed these effects [29] further suggesting ameliorative effects of CRV toward $HgCl_2$-induced apoptosis.

One characteristic that distinguishes the inflammatory response is the creation of proinflammatory cytokines, containing TNF-α, IL-6, and IL-1β, via NF-κB and/or the inflammasome NLRP3 [38]. The NF-κB signaling pathway is one significant mechanism that starts the transcription of NLRP3 [39]. It often undergoes phosphorylation at Ser536, translocates to the nucleus, and increases NLRP3 and IL-1β mRNA synthesis. Moreover, Fann et al. [40] claim that NF-κB is an indispensable downstream target of MAPK signaling, which regulates IL-1β and TNF-α among other inflammatory cytokines. TNF-α and IL-1β, which both inhibit TNF-α and IL-1β expression and trigger innate immunity and ensuing inflammatory responses, are the main drivers of the inflammatory cascade. Several studies have suggested that pathogenic conditions frequently result in prolonged and/or excessive NO generation, the majority of which is caused by iNOS expression [41]. Specifically, iNOS has garnered significant interest because of its vital roles in disorders associated with inflammation. In reaction to physical, chemical, and biological stimuli such as UV radiation exposure, dioxin, and LPS assault, the majority of normal mammalian tissues exhibit modest expression of the COX-2 protein [42]. The byproduct of iNOS, has been shown to control COX-2 expression and prostaglandin synthesis in inflammatory models [43]. Our work has shown that $HgCl_2$ may cause an increase in inflammatory cytokines by activating pathways such as NLRP3, iNOS/COX-2, TNF-α, NF-κB, and IL-1β, which regulate the production of various pro-inflammatory and cytotoxic genes. CRV decreased the level of these inflammatory factors indicating that CRV's lung protective effects also stem from its ability to regulate inflammation. In parallel to our studies, trimetazidine, an anti-ischemic medication, inhibits renal inflammatory stress, and caspase-dependent apoptosis in rats to prevent mercury nephrotoxicity [44]. Overall, antioxidants may be repurposed to suppress oxidative inflammation in rats, hence reducing $HgCl_2$ lung toxicity.

Several critical biological processes, including angiogenesis, death, differentiation, proliferation of cells, and immunological

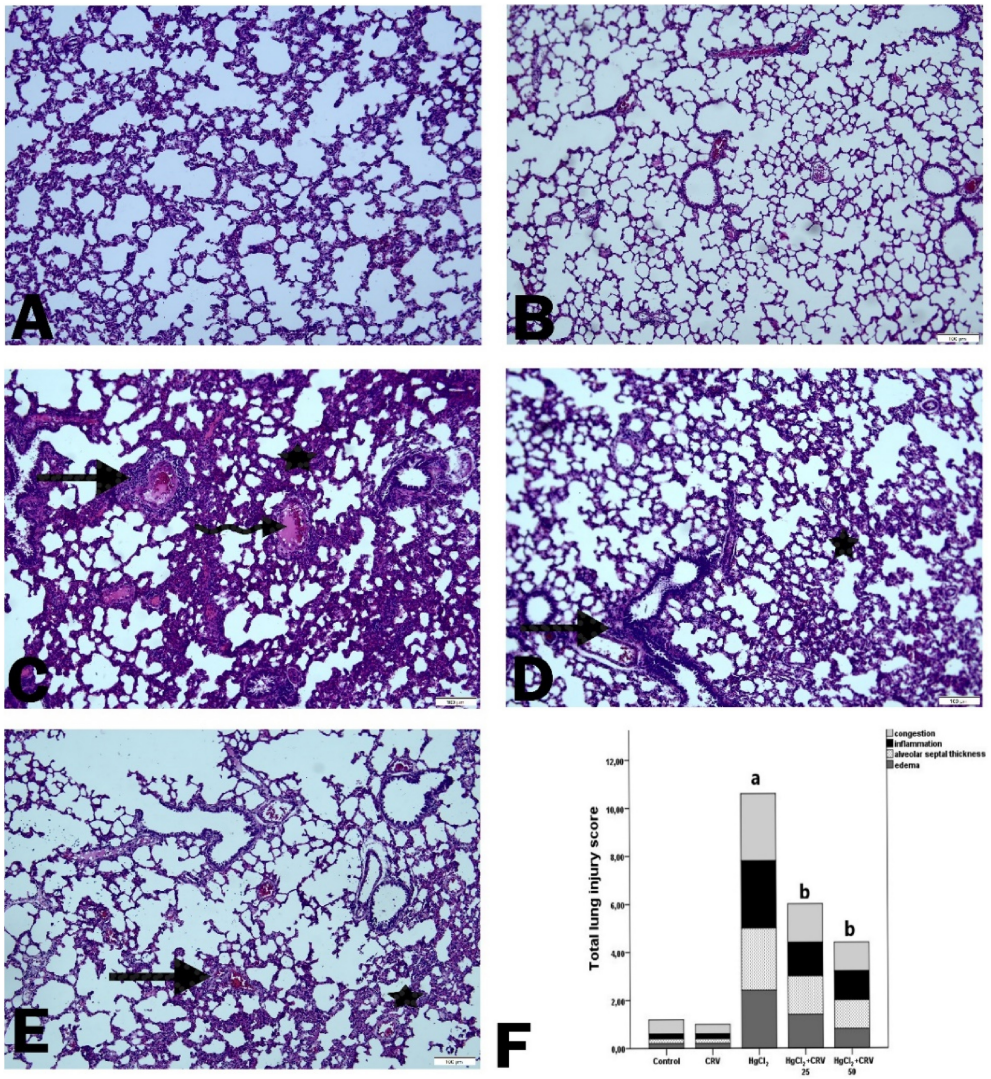

FIGURE 8 | Histological evaluation of hematoxylin–eosin (H&E) stained sections of CRV and $HgCl_2$ treated lung tissues. (A) Control group, (B) CRV group, and (C) $HgCl_2$ group: arrow— inflammatory cell infiltration; curved arrow—congestion; and star—alveolar septal thickness; (D) $HgCl_2$ + CRV 25 group: arrow— inflammatory cell infiltration; star—alveolar septal thickness; (E) $HgCl_2$ + CRV 50 group: arrow—inflammatory cell infiltration; star—alveolar septal thickness. Scale bars: 100 μm. (F) Semi-quantitative lung histopathological scores for animal groups treated with CRV and $HgCl_2$. Data are expressed as mean ± SD. $^{a}p < 0.05$ (compared with control); $^{b}p < 0.05$ (compared with $HgCl_2$).

control, are mediated by the JAK/STAT system [45, 46]. RAGE, a member of the immunoglobulin superfamily with a recent evolutionary background, is encoded in the major histocompatibility complex's Class III region [47]. The only organ with clearly visible high levels of RAGE expression is the lung. However, RAGE expression increases rapidly in inflammatory regions, primarily on inflammatory and epithelial cells [48]. Our findings further demonstrate that lung damage raised the levels of STAT3, RAGE, and JAK2, but that the cells were shielded from this toxicity by CRV treatment. Together, these findings added to the evidence supporting CRV's capacity to inhibit STAT3, RAGE, and JAK2, thus reducing the inflammatory effects brought on by $HgCl_2$.

One important intracellular route for the breakdown and recycling of long-lived proteins and whole organelles is autophagy [49]. The structural proteins of autophagosomal membranes are called LC3s [50]. Three members of the human LC3 gene family—LC3A, LC3B, and LC3C—as well as two different forms of the LC3A protein have been found. One of the primary elements of the autophagosome membrane, which is present in both the inner and outer sites of the membrane, is the form LC3-II. A key function of autophagy, a process of programmed cell survival that is enhanced during times of cell stress and terminated during the cell cycle, is played by Beclin 1, the mammalian orthologue of yeast Atg6 [51]. We used RT-PCR to measure the mRNA transcript levels of LC3A, LC3B, and Beclin-1 to assess their expression levels in order to examine the impact of CRV on $HgCl_2$-induced autophagy in the lungs. Our research showed that CRV treatment in the lung tissue decreased the mRNA transcript levels of LC3A, LC3B, and Beclin-1, which were increased by $HgCl_2$. There are limited studies regarding autophagic effects of $HgCl_2$. In a study, $HgCl_2$ exposure upregulated the expression levels of LC3 proteins were upregulated [52]. In another study, $HgCl_2$ upregulated Beclin-1, LC3A, and LC3B levels in testes [29].

When lung tissue was examined with H&E staining, thickening of the alveolar septum, an increase in inflammatory cells, and an increase in vascular congestion and bleeding showed $HgCl_2$-induced lung injury. It was determined that CRV administered together with $HgCl_2$ caused a significant decrease in alveolar septal thickening, congestion, edema, and inflammatory cell infiltration. The results showed herein demonstrated that CRV treatment reduced the severity of $HgCl_2$-induced lung damage.

5 | Conclusion

In conclusion, our investigation revealed that the treatment with of CRV may be able to counteract and lessen the oxidative stress, apoptosis, autophagy, and inflammation that $HgCl_2$ has caused in lung tissue, as well as shield the lung from the toxicity caused by $HgCl_2$.

Author Contributions

Berna Eriten: methodology, statistical analysis, writing – review and editing, data curation. **Sefa Kucukler:** investigation, methodology, conceptualization. **Cihan Gur:** investigation, methodology, validation, conceptualization. **Adnan Ayna:** writing – review and editing, supervision. **Halit Diril:** writing – review and editing, statistical analysis. **Cuneyt Caglayan:** validation, writing – review and editing, supervision.

Conflicts of Interest

The authors declare no conflicts of interest.

Data Availability Statement

The data that support the findings of this study are available from the corresponding author upon reasonable request.

References

1. S. Kucukler, F. Benzer, S. Yildirim, et al., "Protective Effects of Chrysin Against Oxidative Stress and Inflammation Induced by Lead Acetate in Rat Kidneys: A Biochemical and Histopathological Approach," *Biological Trace Element Research* 199, no. 4 (2021): 1501–1514.

2. C. Caglayan, P. Taslimi, C. Türk, F. M. Kandemir, Y. Demir, and İ. Gulcin, "Purification and Characterization of the Carbonic Anhydrase Enzyme From Horse Mackerel (*Trachurus trachurus*) Muscle and the Impact of Some Metal Ions and Pesticides on Enzyme Activity," *Comparative Biochemistry and Physiology Part C: Toxicology & Pharmacology* 226 (2019): 108605.

3. C. Caglayan, P. Taslimi, C. Türk, et al., "Inhibition Effects of Some Pesticides and Heavy Metals on Carbonic Anhydrase Enzyme Activity Purified From Horse Mackerel (*Trachurus trachurus*) Gill Tissues," *Environmental Science and Pollution Research* 27, no. 10 (2020): 10607–10616.

4. M. Balali-Mood, K. Naseri, Z. Tahergorabi, M. R. Khazdair, and M. Sadeghi, "Toxic Mechanisms of Five Heavy Metals: Mercury, Lead, Chromium, Cadmium, and Arsenic," *Frontiers in Pharmacology* 12 (2021): 643972.

5. İ. Gulcin and S. H. Alwasel, "Metal Ions, Metal Chelators and Metal Chelating Assay as Antioxidant Method," *Processes* 10, no. 1 (2022): 132.

6. N. Mao, J. Antley, M. Cooper, N. Shah, A. Kadam, and A. Khalizov, "Heterogeneous Chemistry of Mercuric Chloride on Inorganic Salt Surfaces," *Journal of Physical Chemistry A* 125, no. 18 (2021): 3943–3952.

7. B. Bharti, H. Li, Z. Ren, R. Zhu, and Z. Zhu, "Recent Advances in Sterilization and Disinfection Technology: A Review," *Chemosphere* 308 (2022): 136404.

8. E. Paduraru, D. Iacob, V. Rarinca, et al., "Comprehensive Review Regarding Mercury Poisoning and Its Complex Involvement in Alzheimer's Disease," *International Journal of Molecular Sciences* 23, no. 4 (2022): 1992.

9. A. V. Skalny, T. R. R. Lima, T. Ke, et al., "Toxic Metal Exposure as a Possible Risk Factor for COVID-19 and Other Respiratory Infectious Diseases," *Food and Chemical Toxicology* 146 (2020): 111809.

10. L. A. Broussard, C. A. Hammett-Stabler, R. E. Winecker, and J. D. Ropero-Miller, "The Toxicology of Mercury," *Laboratory Medicine* 33, no. 8 (2002): 614–625.

11. F. M. Kandemir, C. Caglayan, E. Darendelioğlu, S. Küçükler, E. İzol, and Ö. Kandemir, "Modulatory Effects of Carvacrol Against Cadmium-Induced Hepatotoxicity and Nephrotoxicity by Molecular Targeting Regulation," *Life Sciences* 277 (2021): 119610.

12. T. Alagöz, F. G. Çalişkan, H. G. Bilgiçli, et al., "Synthesis, Characterization, Biochemical, and Molecular Modeling Studies of Carvacrol-Based New Thiosemicarbazide and 1,3,4-Thiadiazole Derivatives," *Archiv der Pharmazie* 356, no. 12 (2023): 2300370.

13. A. Bytyqi-Damoni, A. Kestane, P. Taslimi, et al., "Novel Carvacrol Based New Oxypropanolamine Derivatives: Design, Synthesis, Characterization, Biological Evaluation, and Molecular Docking Studies," *Journal of Molecular Structure* 1202 (2020): 127297.

14. A. Bytyqi-Damoni, E. M. Uc, R. E. Bora, et al., "Synthesis, Characterization, and Computational Study of Novel Carvacrol-Based 2-Aminothiol and Sulfonic Acid Derivatives as Metabolic Enzyme Inhibitors," *Journal of Molecular Structure* 1303 (2024): 137516.

15. T. Ali, S. T. Majeed, R. Majeed, et al., "Recent Advances in the Pharmacological Properties and Molecular Mechanisms of Carvacrol," *Revista Brasileira de Farmacognosia* 34, no. 1 (2024): 35–47.

16. M. O. Yıldız, H. Çelik, C. Caglayan, A. Genç, T. Doğan, and E. Satıcı, "Neuroprotective Effects of Carvacrol Against Cadmium-Induced Neurotoxicity in Rats: Role of Oxidative Stress, Inflammation and Apoptosis," *Metabolic Brain Disease* 37, no. 4 (2022): 1259–1269.

17. C. Gur, S. A. Akarsu, N. Akaras, S. C. Tuncer, and F. M. Kandemir, "Carvacrol Reduces Abnormal and Dead Sperm Counts by Attenuating Sodium Arsenite-Induced Oxidative Stress, Inflammation, Apoptosis, and Autophagy in the Testicular Tissues of Rats," *Environmental Toxicology* 38, no. 6 (2023): 1265–1276.

18. C. Caglayan, F. M. Kandemir, E. Darendelioğlu, S. Yıldırım, S. Kucukler, and M. B. Dortbudak, "Rutin Ameliorates Mercuric Chloride-Induced Hepatotoxicity in Rats via Interfering With Oxidative Stress, Inflammation and Apoptosis," *Journal of Trace Elements in Medicine and Biology* 56 (2019): 60–68.

19. Z. A. Placer, L. L. Cushman, and B. C. Johnson, "Estimation of Product of Lipid Peroxidation (Malonyl Dialdehyde) in Biochemical Systems," *Analytical Biochemistry* 16, no. 2 (1966): 359–364.

20. Y. Sun, L. W. Oberley, and Y. Li, "A Simple Method for Clinical Assay of Superoxide Dismutase," *Clinical Chemistry* 34, no. 3 (1988): 497–500.

21. H. Aebi, "[13] Catalase In Vitro," *Methods in Enzymology* 105 (1984): 121–126.

22. R. A. Lawrence and R. F. Burk, "Glutathione Peroxidase Activity in Selenium-Deficient Rat Liver," *Biochemical and Biophysical Research Communications* 71, no. 4 (1976): 952–958.

23. J. Sedlak and R. H. Lindsay, "Estimation of Total, Protein-Bound, and Nonprotein Sulfhydryl Groups in Tissue With Ellman's Reagent," *Analytical Biochemistry* 25, no. 1 (1968): 192–205.

24. O. H. Lowry, N. J. Rosebrough, A. L. Farr, and R. J. Randall, "Protein Measurement With the Folin Phenol Reagent," *Journal of Biological Chemistry* 193, no. 1 (1951): 265–275.

25. K. J. Livak and T. D. Schmittgen, "Analysis of Relative Gene Expression Data Using Real-Time Quantitative PCR and the $2^{-\Delta\Delta CT}$ Method," *Methods* 25, no. 4 (2001): 402–408.

26. D. Veeraswamy, A. Subramanian, D. Mohan, et al., "Exploring the Origins and Cleanup of Mercury Contamination: A Comprehensive Review," *Environmental Science and Pollution Research* (2023): 1–30.

27. A. O. Asuku, M. T. Ayinla, A. J. Ajibare, and T. S. Olajide, "Mercury Chloride Causes Cognitive Impairment, Oxidative Stress and Neuroinflammation in Male Wistar Rats: The Potential Protective Effect of 6-Gingerol-Rich Fraction of Zingiber Officinale via Regulation of Antioxidant Defence System and Reversal of Pro-Inflammatory Markers Increase," *Brain Research* 1826 (2024): 148741.

28. Y. Liu, X. Guo, L. Yu, et al., "Luteolin Alleviates Inorganic Mercury-Induced Liver Injury in Quails by Resisting Oxidative Stress and Promoting Mercury ion Excretion," *Molecular Biology Reports* 50, no. 1 (2023): 399–408.

29. H. Şimşek, C. Gür, S. Küçükler, et al., "Carvacrol Reduces Mercuric Chloride-Induced Testicular Toxicity by Regulating Oxidative Stress, Inflammation, Apoptosis, Autophagy, and Histopathological Changes," *Biological Trace Element Research* (2023): 1–13.

30. A. M. T. Gusti, S. Y. Qusti, E. M. Alshammari, E. A. Toraih, and M. S. Fawzy, "Antioxidants-Related Superoxide Dismutase (SOD), Catalase (CAT), Glutathione Peroxidase (GPX), Glutathione-S-Transferase (GST), and Nitric Oxide Synthase (NOS) Gene Variants Analysis in an Obese Population: A Preliminary Case-Control Study," *Antioxidants* 10, no. 4 (2021): 595.

31. C. J. Norbury and B. Zhivotovsky, "DNA Damage-Induced Apoptosis," *Oncogene* 23, no. 16 (2004): 2797–2808.

32. D. Kashyap, V. K. Garg, and N. Goel, "Intrinsic and Extrinsic Pathways of Apoptosis: Role in Cancer Development and Prognosis," *Advances in Protein Chemistry and Structural Biology* 125 (2021): 73–120.

33. S. N. Özbolat and A. Ayna, "Chrysin Suppresses HT-29 Cell Death Induced by Diclofenac Through Apoptosis and Oxidative Damage," *Nutrition and Cancer* 73, no. 8 (2021): 1419–1428.

34. K. Engeland, "Cell Cycle Regulation: p53-p21-RB Signaling," *Cell Death and Differentiation* 29, no. 5 (2022): 946–960.

35. A. Alhusaini, S. Alghilani, W. Alhuqbani, and I. H. Hasan, "Vitamin E and Lactobacillus Provide Protective Effects Against Liver Injury Induced by HgCl2: Role of CHOP, GPR87, and mTOR Proteins," *Dose-Response* 19, no. 2 (2021): 15593258211011360.

36. S. S. Ramadan, F. A. El Zaiat, E. A. Habashy, et al., "Coenzyme Q10-Loaded Albumin Nanoparticles Protect Against Redox Imbalance and Inflammatory, Apoptotic, and Histopathological Alterations in Mercuric Chloride-Induced Hepatorenal Toxicity in Rats," *Biomedicine* 11, no. 11 (2023): 3054.

37. P. Wang, Q. Luo, H. Qiao, et al., "The Neuroprotective Effects of Carvacrol on Ethanol-Induced Hippocampal Neurons Impairment via the Antioxidative and Antiapoptotic Pathways," *Oxidative Medicine and Cellular Longevity* 2017 (2017): 4079425.

38. I. S. Afonina, Z. Zhong, M. Karin, and R. Beyaert, "Limiting Inflammation—The Negative Regulation of NF-κB and the NLRP3 Inflammasome," *Nature Immunology* 18, no. 8 (2017): 861–869.

39. Y. Chen, X. Ye, G. Escames, et al., "The NLRP3 Inflammasome: Contributions to Inflammation-Related Diseases," *Cellular & Molecular Biology Letters* 28, no. 1 (2023): 51.

40. D. Y.-W. Fann, Y.-A. Lim, Y.-L. Cheng, et al., "Evidence That NF-κB and MAPK Signaling Promotes NLRP Inflammasome Activation in Neurons Following Ischemic Stroke," *Molecular Neurobiology* 55, no. 2 (2018): 1082–1096.

41. G. Serreli and M. Deiana, "Role of Dietary Polyphenols in the Activity and Expression of Nitric Oxide Synthases," *Antioxidants* 12, no. 1 (2023): 147.

42. A. Murakami and H. Ohigashi, "Targeting NOX, INOS and COX-2 in Inflammatory Cells: Chemoprevention Using Food Phytochemicals," *International Journal of Cancer* 121, no. 11 (2007): 2357–2363.

43. F. Cianchi, F. Perna, and E. Masini, "iNOS/COX-2 Pathway Interaction: A Good Molecular Target for Cancer Treatment," *Current Enzyme Inhibition* 1, no. 2 (2005): 97–105.

44. A. Sedky and A. C. Famurewa, "Anti-Ischemic Drug Trimetazidine Blocks Mercury Nephrotoxicity By Suppressing Renal Redox Imbalance, Inflammatory Stress And Caspase-Dependent Apoptosis In Rats," *Drug and Chemical Toxicology* (2023): 1–8.

45. Q. Pang, L. You, X. Meng, et al., "Regulation of the JAK/STAT Signaling Pathway: The Promising Targets for Cardiovascular Disease," *Biochemical Pharmacology* 213 (2023): 115587.

46. A. Hjazi, R. F. Obaid, S. S. Ali, et al., "The Cross-Talk Between LncRNAs and JAK-STAT Signaling Pathway in Cancer," *Pathology, Research and Practice* 248 (2023): 154657.

47. R. Kang, D. Tang, M. T. Loze, and I. I. I. H. J. Zeh, "Apoptosis to Autophagy Switch Triggered by the MHC Class III-Encoded Receptor for Advanced Glycation Endproducts (RAGE)," *Autophagy* 7, no. 1 (2011): 91–93.

48. M.-C. Chen, K.-C. Chen, G.-C. Chang, et al., "RAGE Acts as an Oncogenic Role and Promotes the Metastasis of Human Lung Cancer," *Cell Death and Disease* 11, no. 4 (2020): 265.

49. T. Lamark and T. Johansen, "Mechanisms of Selective Autophagy," *Annual Review of Cell and Developmental Biology* 37, no. 1 (2021): 143–169.

50. T. Nishimura and S. A. Tooze, "Emerging Roles of ATG Proteins and Membrane Lipids in Autophagosome Formation," *Cell Discovery* 6, no. 1 (2020): 32.

51. S. Kaur and H. Changotra, "The Beclin 1 Interactome: Modification and Roles in the Pathology of Autophagy-Related Disorders," *Biochimie* 175 (2020): 34–49.

52. L. Gu, F. Jin, T. Yang, et al., "Mercuric Chloride Induced Brain Toxicity in Mice: The Protective Effects of Puerarin-Loaded PLGA Nanoparticles," *Journal of Biochemical and Molecular Toxicology* 37, no. 10 (2023): e23425.